IOSR Journal of Electrical and Electronics Engineering (IOSR-JEEE)
e-ISSN: 2278-1676, p-ISSN: 2320-3331, Volume 16, Issue 5 Ser. I (Sep. – Oct. 2021), PP 01-09
www.iosrjournals.org

On The Effect of Hydrothermal Temperature Treatment on the Phase Structure, Morphology and Optical Properties of TiO_2 Nanoparticles

Asmaa Dahy [1], M. Dongol [2], A. A. Ebnalwaled [1,3*]
[1] *Electronics & Nano Devices Lab, Physics Department, Faculty of Science, South Valley University, Qena, 83523 Egypt.*
[2] *Nano & Thin Film Lab, Physics Department, Faculty of Science, South Valley University, Qena, 83523 Egypt.*
[3] *Faculty of Nanotechnology for Postgraduate Studies, Cairo University, Sheikh Zayed Campus, 6th October City, Giza, 12588, Egypt*
kh_ebnalwaled@yahoo.com

Abstract
In the current work, the morphology, structure, and optical properties of TiO_2 nanoparticles were studied to examine the effect of hydrothermal temperatures treatment on the nanoparticle's properties. The prepared TiO_2 nanoparticles were analyzed by X-ray diffraction (XRD), high-resolution electron microscopy (HR-TEM), Fourier-transforming infrared spectroscopy (FTIR), and Ultraviolet-Visible (UV-Vis) spectrophotometers. Hydrothermal treatment leads to a crystalline transition from the anatase phase to the monoclinic phase in the commercial nanoparticles of TiO_2 and decreases the particle size. Results from the HR-TEM indicated that a nanosheet was observed in comparison to commercial TiO_2 nanoparticles after hydrothermal treatment. Analysis of UV-Vis revealed that the transmission and absorption of TiO_2 samples treated with different hydrothermal reaction temperatures were changed compared to the original sample. Taken together, hydrothermal temperature treatment signifies the morphology, structure, and optical properties of TiO_2.

Keywords: *nanostructure, TiO_2, anatase, bronze, hydrothermal treatment.*

Date of Submission: 20-08-2021 Date of Acceptance: 05-09-2021

I. Introduction

Titanium dioxide (TiO_2) nanomaterial is commonly regarded as a photocatalyst due to elevated levels of oxidation, nontoxicity, photoactivity, high chemical photostable levels and human and environmental safety [1-3]. A variety of applications, including solar cells, self-wash structure, water restoration, pollutant depletion, battery, and chemical sensors, are widely used in TiO_2 photocatalytic [4-6]. The photocatalytic behavior of TiO_2 nanostructures has been reported to be related to their particle size, specific surface area, morphology, and the synthesis process regulated by crystal structure [7, 8]. Therefore, TiO_2, as a photoelectrode material for solar cells of third generation, shows comparatively high efficiency [9]. Their functional capabilities have also not been studied directly, but they are thought to have a large potential as functional materials [10]. Consequently, it is essential to improve the method for selectively synthesizing superior properties of TiO_2 polymorphs.

Under ambient conditions, TiO_2 exists in eight polymorphs include rutile, anatase, and brookite which are in natural polymorphs. Other polymorphs include TiO_2 (B) (bronze), TiO_2 (H) (hollandite), and the other three polymorphs can only be produced synthetically in the laboratory [11, 12]. The TiO_2 polymorphic band gap energy varies from 3.0 to 3.4 eV, which directly influences the band structure of each of the phases [13]. Due to their stability and easy synthetization, anatase and rutile forms have the widest practical applications. However, there are only a limited number of methods for the single-phase synthesis of the other polymorphs forms, including brookite and TiO_2 (B) [11]. Certain methods for the synthesis of TiO_2 nanoparticles include the sol-gel process, hydrothermal synthesis, the metal-organic chemical vapor deposition (MOCVD), flame combustion, and electrochemical anodization [14] are used. There are numerous benefits for hydrothermal techniques because the process is simple, economical, and very low-temperature nanoparticles can be prepared [15]. The production of TiO_2 nanostructure is determined by the conditions of synthetization (pressure, reaction temperature, reaction time, the initial amount of TiO_2 and sodium hydroxide (NaOH) concentration, acid washing and calcination [8, 16]. By adjusting the synthesis conditions, the single phase and the morphological control of titania crystals can be obtained. Therefore, hydrothermal temperature is considered as an effective

parameter for controlling the growth process and properties of TiO_2 nanoparticles. So the aim of this study is to investigate the effect of hydrothermal temperature treatment on the phase structure, morphology and optical properties of TiO_2 nanoparticles, which will open the door for more application of TiO_2 nanoparticles.

II. Materials And Methods

2.1. Chemical reagents for the synthesis of TiO_2

Titanium dioxide extra pure (purity 98%) was purchased from Loba Chemie Pvt, India. Sodium Hydroxide Anhydrous NaOH extra pure grade (purity 98%) was purchased from Top Chem, Egypt. Both reagents were used as received without further purification. Hydrochloric acid (HCl) (ADWIC, El-Nasr Pharmaceutical Chemicals co., Egypt) at concentration of 30-34% was used for washing and furthermore with distilled water.

2.2. Synthesis of TiO_2 nanoparticles

Figure 1 shows a schematic diagram for the synthesis of TiO_2 nanoparticles.

First step (Mixing): 1.5 g of commercial TiO_2 (16. 79 nm, S1) was mixed with 60 mL of 10M NaOH. The mixture further was stirred for 20 min in a beaker (dipped in acetone and alcohol, and then rinsed with distilled water). The mixture was then transferred to Teflon-lined autoclave (hydrothermal reactor). The autoclave was placed in a preheated electric oven at different temperatures (110 (S2), 150 (S2), or 170 ºC (S3)) for 24 h under autogenously pressure and static conditions, and then air-cooled to room temperature.

Second step (Acid washing): The obtained products were collected and washed with dilute HCl (pH 1.6) for 24 h to remove most of NaOH.

Third step (Washing): The precipitate was further washed with distilled water until the pH of the supernatant was close to 7.

Fourth step (Calcination): The obtained powder was calcinated at 450 ºC for 2 h.

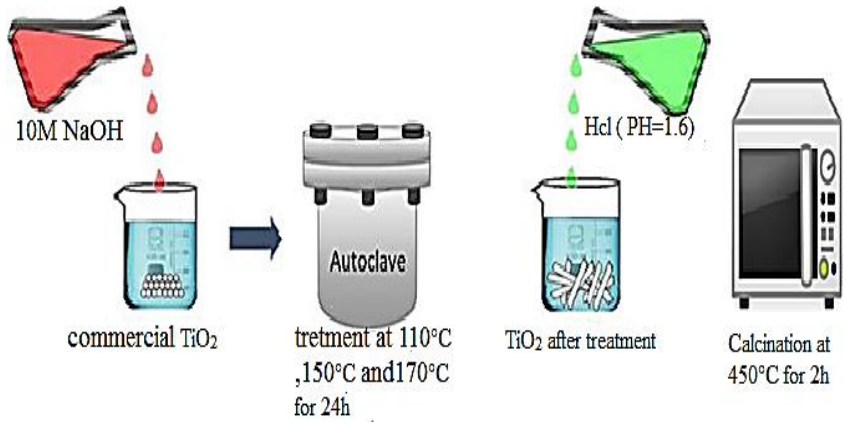

Figure 1. Hydrothermal method used to prepare TiO_2 nanoparticles at different reaction temperatures**.**

2.3. Materials Characterization

After treatment of TiO_2 by hydrothermal method at different temperature, various techniques were used to evaluate their structure, morphology, and optical properties. In this study, we analyzed the TiO_2 samples using X-ray diffraction (XRD) pattern data at room temperature for powder samples of TiO_2 by a PANalytical X'Pert powder Cu-kα radiation (λ=1.54056 Å). The morphologies of the samples (S1, S2, S3, and S4) were detected by high resolution transmission electron microscopy (HR-TEM) (JEOL, JEM-2100 – Japan). The Fourier-transform infrared spectroscopy (FT-IR) technique (Jasco Model 4100 – Japan) was used to characterize the bond structure of the TiO_2 nanoparticles. Furthermore, the optical properties were characterized by using UV-Vis Spectrophotometer (analytic Jena, specord 200 plus, Germany).

III. Results and Discussion

3.1. Crystallinity and phase identification

The XRD patterns of the prepared TiO_2 powders under different hydrothermal temperatures and the commercial TiO_2 without any modifications are shown in figures (2 a & b). The XRD pattern results revealed the overall crystalline structure and phase purity of the TiO_2. Figure (2 a) shows most of the peaks in S1 and S2 could be recorded as anatase (A) TiO_2, which are essentially in approval with the reported values [File Card No: 01-089-4203] [17]. Nevertheless, the diffraction peaks of Rutile (R) can also be found in S1, but only Rutile {R (110),(301)} can also be found in S2 and approved with the reported values [File Card No: 00-002-0494] [18]. These results suggest that the peaks{R(101),(2200} vanish and all peaks in S1 and S2 are with a tetragonal structure.

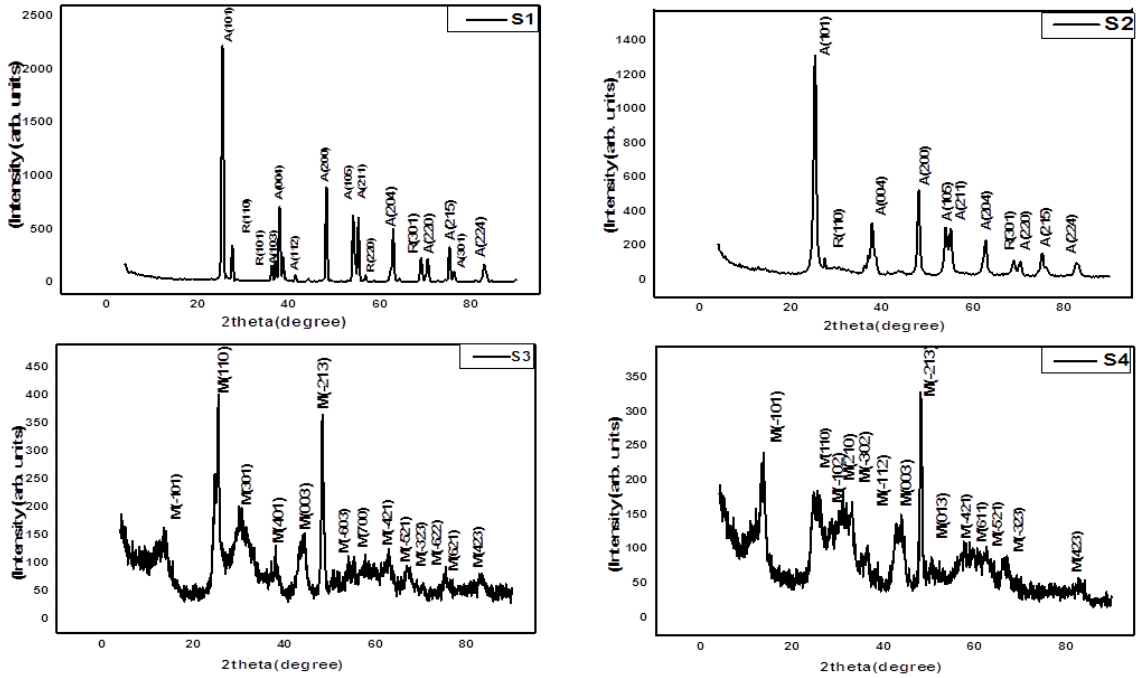

Figure 2. XRD of commercial TiO_2 sample and hydrothermally treated at 110, 150 and 170 °C respectively.

The bulk of the fields in figure (2 b) can be shown as TiO_2 monoclinic (M) in S3 and S4 which basically are reversed by the values [File Card No:03-065-1156] [19]. Raising the temperature of the hydrothermal could increase the number of peaks in S3 and S4. In addition, increasing the temperature for hydrothermal TiO_2 lead to a transition in the top location as some peaks moved marginally to an elevated angel, such as the top of plane M (301) and M (-302). Hydrothermal treatment causes a change in the structure of S1 as shown by XRD analysis. Increasing the hydrothermal temperature could decrease the sharpness and the amplitude of the peaks for S2, S3 and S4 indicating a low crystallinity of TiO_2 nanoparticles compared with S1. The XRD spectrum reveals that the S3 and S4 are polycrystalline in nature having monoclinic structure. As shown from the XRD patterns, each peak has a finite width. The inter-planer spacing d for every peak was calculated according to the Bragg law:

$$n\lambda = 2d \sin\Theta \qquad (1)$$

where n is an integer determined by the order of diffraction (n=1); λ is the wavelength of x-rays, (λ = 1.541838Å); d is the spacing between the planes in the atomic lattice, and θ is the angle between the incident ray and the scattering planes. The lattice parameters of anatase, monoclinic TiO_2 were calculated using unit cell software. The method and implementation are described by Holland [20].
The formula for tetragonal system is:

$$\frac{1}{d^2} = \left\{\frac{(h^2+k^2)}{a^2}\right\} + \left(\frac{l^2}{c^2}\right) \qquad (2)$$

$$a = b \neq c,\ \alpha = \beta = \gamma = 90$$

The formula for monoclinic system is:

$$\left(\frac{1}{d^2}\right) = \frac{1}{(sin^2\beta)}\left\{\left(\frac{h^2}{a^2}\right) + \left(\frac{k^2 sin^2\beta}{b^2}\right) + \left[\left(\frac{l^2}{c^2}\right) - \left(\frac{2hl\ cos\beta}{ac}\right)\right]\right\} \qquad (3)$$

$$a \neq b \neq c,\ \alpha = \gamma = 90 \neq \beta$$

The lattice parameters of TiO_2 synthesized at different hydrothermal temperatures are shown in tables 1&2. Crystallite size (**D**) of the obtained TiO_2 was calculated from the Debye –Scherrer's formula as shown in table 3.

$$D = \left(\frac{0.9\times\lambda}{\beta\ \cos\theta}\right) \qquad (4)$$

Crystallite size is decreased by increasing the hydrothermal temperature (figure 3).

Table 1. Lattice parameters of commercial TiO_2 and treated hydrothermal at 110° C.

Calculated Lattice parameters (°A)			Lattice Parameters from standard card no 01-089-4203 Anatase
	TiO_2 commercial	TiO_2 at 110° C	
a = b	3.77757	3.78548	3.785
c =	9.48347	9.49533	9.514

Table 2. Lattice parameters of TiO_2 treated hydrothermal at 150° C and 170° C.

Calculated Lattice parameters (°A)			Lattice Parameters from standard card no 03-065-1156 Monoclinic
	TiO_2 at 150° C	TiO_2 at 170° C	
a =	12.24163	12.11203	12.1787
b =	3.72763	3.76586	3.7412
c =	6.51727	6.53184	6.5249
β=	107.70021	107.49103	107.05
Vol cell	283.3189	284.1566	284.23

Table 3. TiO_2 particle size values at different synthesize conditions.

Sample name	Condition	Phase	D (nm)
S1	Commercial	Tetragonal	16.79
S2	Treated at 110°C	Tetragonal	11.61
S3	Treated at 150°C	Monoclinic	5.55
S4	Treated at 170°C	Monoclinic	3.95

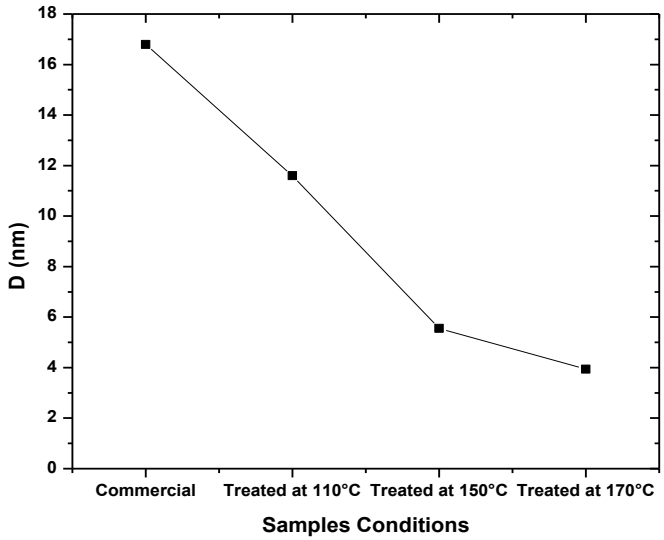

Figure 3. TiO_2 particle size values at different preparation conditions.

3.2. FT-IR spectra for TiO_2

The FT-IR is obtained as transmission spectra of the KBr sample pellets to characterize the bond structure of the TiO_2 nanoparticles. Figure (4) shows the FT-IR of the TiO_2-NPs prepared by hydrothermal method at different reaction temperatures (S2, S3, and S4) and S1 in the range of 4000 to 400 cm^{-1}. Four absorption bands are observed in all samples, the first peak is appeared between 3700 to 3000 cm^{-1} and it belongs to stretching hydroxyl (O-H), representing the water as moisture. The second peak is observed between 2400 and 2300 cm^{-1}, and this absorption band was likely related to the stretching vibrations bonds C=O and (O–H) respectively, existing between the adsorbed water molecules and indicating the higher amount of hydroxyl group. The third peak is observed between 1700 and 1600 cm^{-1}, and it belongs to stretching of titanium carboxylate. The fourth one in the spectrum between 800 and 450 cm^{-1} is assigned to Ti-O stretching bands [22].

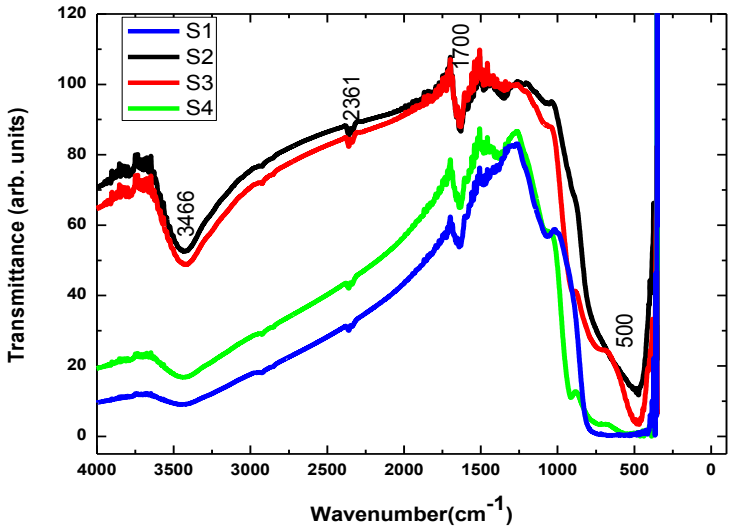

Figure 4. FTIR analyses for TiO_2 nanoparticles (S1, S2, S3, and S4)

3.3. Morphology of TiO_2

The HR-TEM was employed to obtain direct information about the shape and the size of the TiO_2 nanoparticles. It is known that in HR-TEM technique, the interference between the transmitted and the scattered beams produce an interference image. As shown from figure (5), it has been found that the different reaction temperatures could influence the shape and the size of the original commercial TiO_2 nanoparticles. From figure 5 S1 sample appears in a spherical particle form. While, increasing the hydrothermal reaction temperatures from 110 ºC to 170 ºC causes a change in the TiO_2 nanoparticles from tube shape to the sheet form, as well as a decrease in their particle size. The average size of all samples in the range of 3-20 nm which approximately is in close agreement with the results obtained from the powder.

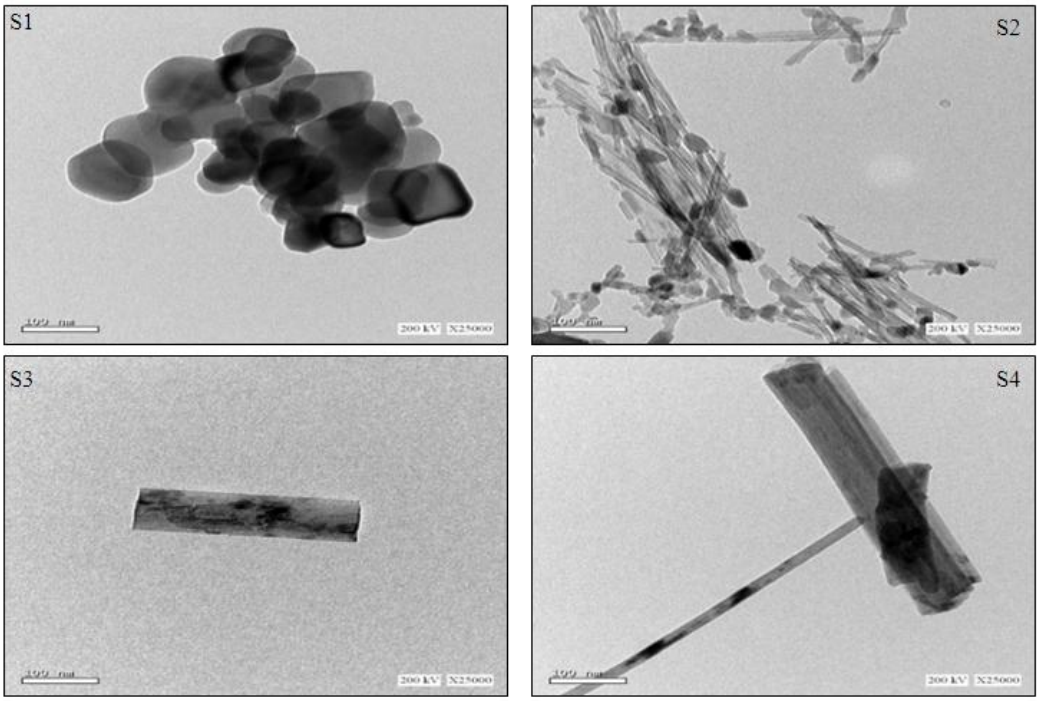

Figure 5. HR-TEM for TiO_2 samples at different preparations conditions

3.4. Optical properties of TiO_2

3.4.1. Optical properties

In general, the interaction between any materials and incident light leads to a maximum absorption at a particular wavelength. In the current work, the absorption spectrum is given by suspending nano-powders of TiO_2 in a distilled water at room temperature using UV-visible spectroscopy. Figure (6 a) illustrate the transmittance for all samples. From the figure, it is evident that different hydrothermal reaction temperatures of TiO_2 nanoparticles affected the transmission of the samples with compared to the original sample before hydrothermal effect. S2 has relatively a higher transmission along the visible wavelengths. Subsequently, S3 has transmission value less than the values of S4 and S1. Figure (6 b) shows the absorbance spectra of TiO_2 nanoparticles samples over a spectral ranging between 200 to 1100 nm. For TiO_2 nanoparticles, the absorption edge is observed to be shifted towards longer wavelengths with the increase of reaction temperature from 110 ºC to 150 ºC (figure 6 b). This means that the absorption band of TiO_2 nanoparticles is shortened to near UV's wavelengths and resulted in a narrow absorption band. The absorption edge of TiO_2 nanoparticles has precisely measured and found to be 255 nm at S2 and increased in S3 to reach a value of 275 nm. These are much lower values than that reported for TiO_2 in its bulk form which has a value of 374.9 nm. On the other hand, the absorption edge value of S1 and S4 are not changed with the increase of reaction temperature to 170 ºC and has a value around 297 nm. It is much lower value compared to that of the bulk TiO_2 (374.9 nm).

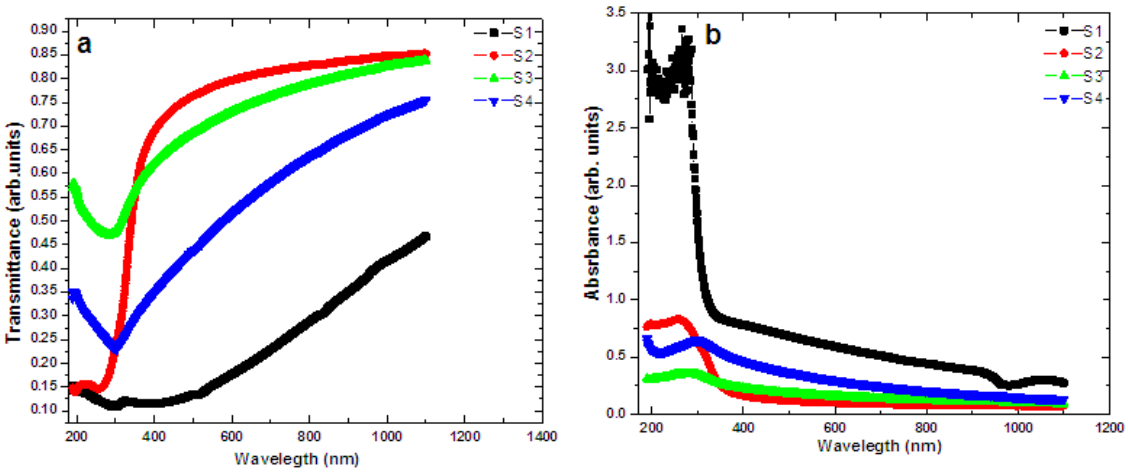

Figure 5. Transmission (**a**) and absorption (**b**) for TiO_2 Samples.

The optical band gap with direct transition can be calculated from the following relationship [21].

$$\alpha h\nu = B(h\nu - E_g)^n \qquad (5)$$

where hν is a photon energy and B is a parameter which depends on the transition probability, α is the absorption coefficient, Eg is the optical band gap and n is a number characterizing the transition process which may take values of 1/2 and 3/2 for direct allowed and forbidden transitions, respectively. The direct band gap energy (Eg) of the TiO_2 samples is determined by fitting the absorbance data to the direct transition equation

$$\alpha h\nu = B(h\nu - E_g)^{\frac{1}{2}} \qquad (6)$$

Figure (7, a-d) shows the plotting of $(\alpha h\nu)^2$ as a function of photon energy hν. The values of the optical band gap E_g for the prepared TiO_2 nanoparticles was calculated. Based on the optical measurements, the Eg values of TiO_2 were found to be (3.72, 3.62, 3.18 and 3.06) eV for S1, S2, S3, and S4, respectively.

This means that the energy band gap is decreased with the increase of the hydrothermal reaction time. Further, the decrease in the crystalline size has found to be accompanied by the decreasing in the energy band gap.

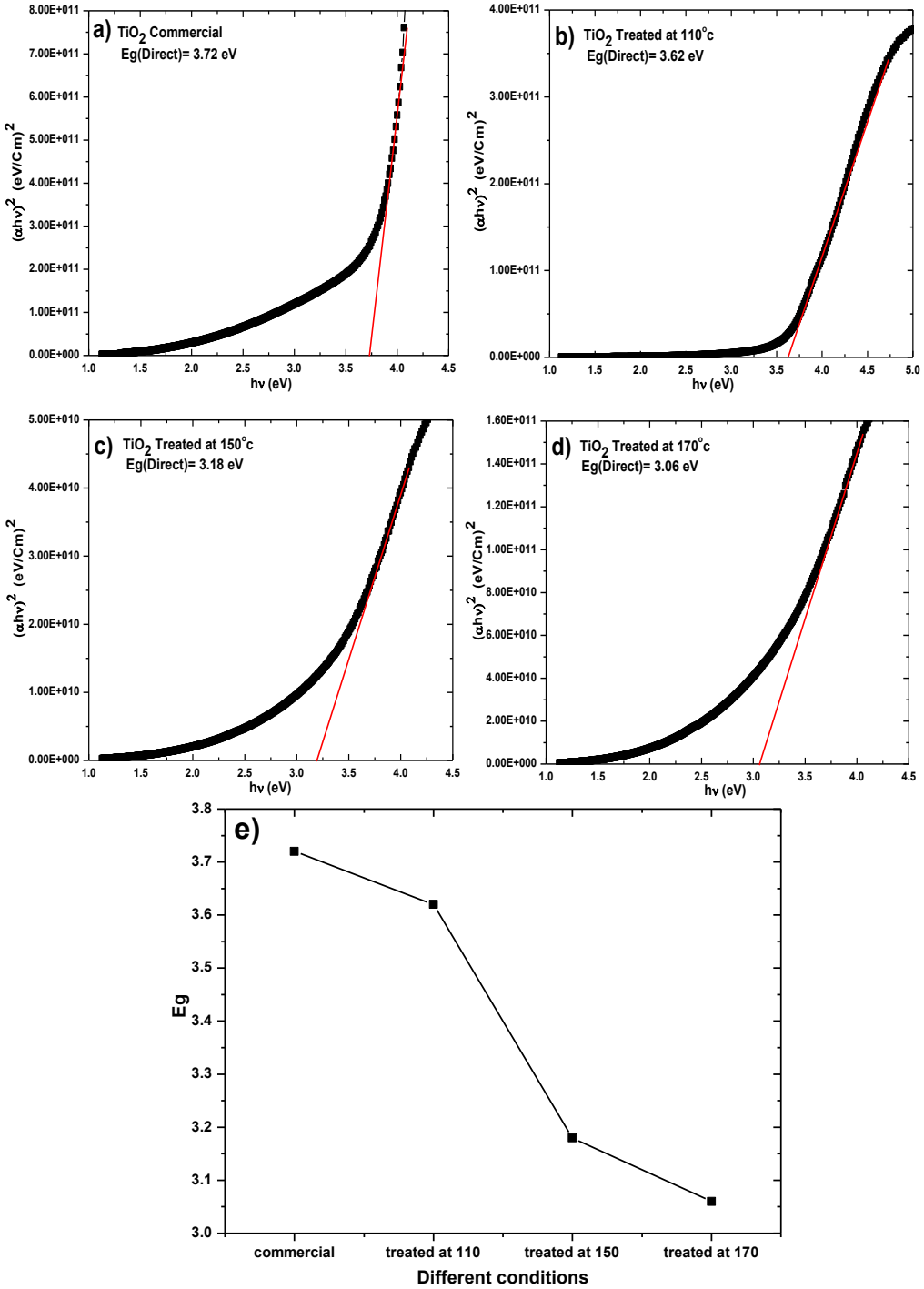

Figure 6. **a**, **b**, **c**, and **d**) $(\alpha h\nu)^2$ vs. hν, **e**) E_g vs. different preparation conditions of TiO_2 samples.

IV. Conclusion:

In the present paper, TiO_2 nanoparticles were prepared under different hydrothermal temperature treatment (110 ºC, 150 ºC and 170 ºC) and compared with the original commercial TiO_2 nanoparticles. We summarized our results that the hydrothermal temperature affects the crystalline phases of the TiO_2 nanoparticles. In addition, HR-TEM showed that the morphology of TiO_2 nanoparticles can be controlled by the treated temperature. UV-Vis analysis showed that different hydrothermal reaction temperatures of TiO_2 nanoparticles could affect the transmission and absorbance of the TiO_2 nanoparticles.

References:

[1]. M Abdelhamid Shahat, F M El-Hossary, Ahmed Ghitas, A M Abd El-Rahman and A. A. Ebnalwaled, Low-temperature Hydrothermal Synthesis of Titanium Dioxide Nanoparticles for Photocatalytic Applications, IOP Conf. Series: Materials Science and Engineering 1171 (2021) 012008 doi:10.1088/1757-899X/1171/1/012008.

[2]. Salem, W., El-Deen, F.N., Ebnalwaled, K. Badry. M, Abdel Latef. A. A., UV‐Induced Antibacterial Activity of Green‐Synthesized TiO_2 Nanoparticles for the Potential Reuse of Raw Surface and Underground Water, *J Plant Growth Regul* (2021). https://doi.org/10.1007/s00344-021-10391-6

[3]. Baloyi, S. and J. Moma, Modified Titanium Dioxide for Photocatalytic Applications. 2019.

[4]. Guo, Q., et al., Fundamentals of TiO_2 Photocatalysis: Concepts, Mechanisms, and Challenges. Advanced Materials, 2019. **31**(50): p. 1901997.

[5]. Nakata, K. and A. Fujishima, TiO_2 photocatalysis: design and applications. J Photochem Photobiol C C13:169-189. Journal of Photochemistry and Photobiology C: Photochemistry Reviews, 2012. **13**: p. 169–189.

[6]. Topçu Şendoğdular, S., G. Jodhani, and P. Gouma, Optimized Nanostructured TiO_2 Photocatalysts. Frontiers in Materials, 2016. **3**.

[7]. Zhang, M., T. Chen, and Y. Wang, Insights into TiO_2 polymorphs: highly selective synthesis, phase transition, and their polymorph-dependent properties. RSC Advances, 2017. **7**(83): p. 52755-52761.

[8]. Shahrezaei, M., et al., Study of synthesis parameters and photocatalytic activity of TiO_2 nanostructures. Journal of Experimental Nanoscience, 2016: p. 1-17.

[9]. Buatong, N., I.M. Tang, and W. Pon-On, Quantum dot-sensitized solar cells having 3D-TiO_2 flower-like structures on the surface of titania nanorods with CuS counter electrode. Nanoscale research letters, 2015. **10**: p. 146-146.

[10]. Mo, S.-D. and W.Y. Ching, Electronic and optical properties of three phases of titanium dioxide: Rutile, anatase, and brookite. Physical Review B, 1995. **51**(19): p. 13023-13032.

[11]. Kobayashi, M., H. Kato, and M. Kakihana, Synthesis of Titanium Dioxide Nanocrystals with Controlled Crystal- and Micro-Structures from Titanium Complexes. Nanomaterials and Nanotechnology, 2013. **3**: p. 23.

[12]. Takahashi, Y., N. Kijima, and J. Akimoto, Synthesis, Structural Change upon Heating, and Electronic Structure of Ramsdellite-Type TiO2. Chemistry of Materials, 2006. **18**(3): p. 748-752.

[13]. Chimupala, Y. and R. Drummond-Brydson. Hydrothermal Synthesis and Phase Formation Mechanism of TiO_2 (B) Nanorods via Alkali Metal Titanate Phase Transformation. in Solid State Phenomena. 2018. Trans Tech Publ.

[14]. Nyamukamba, P., et al., Synthetic Methods for Titanium Dioxide Nanoparticles: A Review. 2018.

[15]. Malligavathy, M., et al., Role of hydrothermal temperature on crystallinity, photoluminescence, photocatalytic and gas sensing properties of TiO_2 nanoparticles. Pramana, 2018. **90**(4): p. 44.

[16]. Zavala, M.Á.L., S.A.L. Morales, and M. Ávila-Santos, Synthesis of stable TiO_2 nanotubes: effect of hydrothermal treatment, acid washing and annealing temperature. Heliyon, 2017. **3**(11): p. e00456.

[17]. Cromer, D.T. and K. Herrington, The Structures of Anatase and Rutile. Journal of the American Chemical Society, 1955. **77**(18): p. 4708-4709.

[18]. Weiser, H.B. and W.O. Milligan, X-ray Studies on the Hydrous Oxides. IV. Titanium Dioxide. The Journal of Physical Chemistry, 1934. **38**(4): p. 513-519.

[19]. Feist, T.P. and P.K. Davies, The soft chemical synthesis of TiO2 (B) from layered titanates. Journal of Solid State Chemistry, 1992. **101**(2): p. 275-295.

[20]. Holland, T.J.B. and S.A.T. Redfern, Unit cell refinement from powder diffraction data; the use of regression diagnostics. Mineralogical Magazine, 1997. **61**(1): p. 65-77.

[21]. Pankove, J.I., Optical processes in semiconductors. 1971, Courier Corporation.

[22]. Kondo, T., P. Rytczak, and S. Bielecki, Bacterial nanocellulose characterization, in Bacterial Nanocellulose. 2016, Elsevier. p. 59-71.

Asmaa Dahy, et. al. "On the Effect of Hydrothermal Temperature Treatment on the Phase Structure, Morphology and Optical Properties of TiO_2 Nanoparticles." *IOSR Journal of Electrical and Electronics Engineering (IOSR-JEEE)*, 16(5), (2021): pp. 01-09.